27

Buoyancy Fluxes in a Stratified Fluid

G. N. Ivey, J. Imberger and J. R. Koseff

Abstract

Direct numerical simulations of the time evolution of homogeneous stably stratified shear flows have been performed for mean flow Richardson numbers in the range from 0.075 to 1.00 and for Prandtl numbers ranging from 0.1 to 2. The local or instantaneous results indicate that when the turbulent Froude number $Fr_T = 1$ the peak value of mixing efficiency is $R_f \approx 0.25$, a result independent of the Prandtl number Pr and thus inconsistent with previous laboratory measurements at values of the Pr of 0.7 and 700. The results are consistent, however, with previous laboratory observations in demonstrating that the mixing efficiency R_f decreases rapidly away from this peak value at $Fr_T = 1$. Using data from both numerical simulations and laboratory experiments with both shear and grid generated turbulence, simple empirical relationships are developed to estimate R_f, and hence buoyancy flux b, for the entire range extending from active turbulence down to the limit where the effects of viscosity and/or density stratification suppress the vertical buoyancy flux.

Introduction

Specification of the turbulent buoyancy flux in a fluid with a stable density gradient is essential to our understanding of mixing processes in a wide variety of geophysical applications. Quantifying the rate of vertical mixing in an ocean or lake is central to parameterizing the transport of heat, salt, and passive tracers. For flows with turbulence driven by a mean shear, for example, this has led to the development of numerous closure models which express eddy diffusivities in terms of the instantaneous mean flow Richardson number Ri (e.g., Pacanowski and Philander, 1981). Such closure schemes rely on data obtained from laboratory and field measurements, although measurements are obtained in fundamentally different ways in the two cases. In the laboratory, data is typically derived from long time averages in steady mean flows, whereas in the field the flow is locally sampled by either horizontal or, more commonly, vertical profiling instruments with a limited number of casts available to obtain ensemble averaged statistics of the turbulence properties. These differences between laboratory and field procedures raise many fundamental questions in regard to parameterizing the turbulence, such as the relationship between mixing rates and mean flow properties and how to correctly account for time variability. If we use local or instantaneous measurements, how

Physical Processes in Lakes and Oceans
Coastal and Estuarine Studies Volume 54, Pages 377-388

are quantities such as the overturning lengthscale L_C, the dissipation rate ε and the buoyancy flux b related? If we only have single or limited numbers of realizations for L_C and ε in the field or laboratory, can we use these to predict b, and with what accuracy? From an energetics point of view, what is the efficiency of conversion of available turbulent kinetic energy to buoyancy flux b?

Ivey and Imberger (1991) examined the efficiency of this energy conversion by introducing a generalized definition of the flux Richardson number R_f, based on the full turbulent kinetic energy equation. Using data from laboratory studies where turbulence was generated by grids (Stillinger et al., 1983; Itsweire et al., 1986; Lienhard et al., 1990) and in studies where turbulence was generated by both a grid and a mean shear (Rohr et al., 1988), they argued that two dimensionless numbers were necessary and sufficient to characterize the mixing (cf Gibson, 1980, 1991), and suggested the use of the turbulent Froude number Fr_T and turbulent Reynolds number Re_T. Their results demonstrated that for fluids with a Prandtl number of 700 the peak value of R_f was 0.20, while for fluids with Prandtl number of 0.7 the peak value of R_f was 0.15. The data also demonstrated a very strong dependence of R_f on the turbulent Froude number Fr_T, with peak values of R_f observed near $Fr_T = 1$ and a rapid decrease of R_f for values of Fr_T either above or below this value. Imberger and Ivey (1991) further demonstrated the value of Fr_T varied greatly in field measurements. When combined with the results of the laboratory observations described above, this has significant implications when computing the buoyancy flux or eddy diffusivity from microstructure measurements of dissipation in the field.

Holt, Koseff and Ferziger (1992) and Itsweire, Koseff, Ferziger and Briggs (1993) examined a sheared stratified flow using direct numerical simulation (DNS) to study the temporal evolution of turbulence in a flow with constant mean density and velocity gradients. Using the pseudospectral method, they solved the Boussinesq form of the Navier Stokes equations for the three dimensional velocity and density fields on a 128^3 grid. The calculations were initialized by specifying pulse initial energy spectra for the turbulent velocity fluctuations (initially isotropic), while the initial fluctuating potential energy was set to zero. The advection imposed by the mean field was removed, leading to equations for the fluctuating quantities, although the imposed *mean* density and velocity gradients were held constant at each time step. Using the code described by Holt et al (1992), in the present study we have undertaken a series of numerical runs at values of the mean Richardson number $Ri = N^2/S^2$ in the range from 0.075 to 1.0, where N is the buoyancy frequency and S the mean shear rate, and with Prandtl numbers Pr ranging from 0.1 to 2 (computational restrictions limit the calculations to small Pr). Below we use the ensemble averaged measurements over the 128^3 point domain from the numerical results at each time step, compare these results with the earlier laboratory results described by Ivey and Imberger (1991), and develop expressions for mixing efficiency R_f and buoyancy flux b in terms of local or instantaneous quantities.

Governing parameters

The turbulent kinetic energy equation may be written as

$$m = b + \varepsilon \tag{1}$$

where ε is the rate of dissipation of turbulent kinetic energy, b denotes the buoyancy flux and m refers to the net mechanical energy required (or available) to sustain the turbulent

motions from all possible sources, including unsteady terms. Following Ivey and Imberger (1991), the mixing efficiency is quantified by the generalized flux Richardson number

$$R_f = \frac{b}{m} = \frac{1}{1+\varepsilon/b} \tag{2}$$

The small scale or turbulent Froude number is defined as

$$Fr_T = \left(\frac{\varepsilon}{N^3 L_C^2}\right)^{1/3} = \left(\frac{L_O}{L_C}\right)^{2/3} \tag{3}$$

where L_C is the centred displacement scale, $L_O = (\varepsilon/N^3)^{1/2}$ is the Ozmidov scale, and N is the buoyancy frequency characterizing the stable background stratification. The turbulent Reynolds number Re_T and the small scale Froude number Fr_γ are defined by

$$Re_T = \left(\frac{\varepsilon L_C^4}{\nu^3}\right)^{1/3} = \left(\frac{L_C}{L_K}\right)^{4/3} \tag{4}$$

$$Fr_\gamma = \left(\frac{\varepsilon}{\nu N^2}\right)^{1/2} = \left(\frac{L_O}{L_K}\right)^{2/3} \tag{5}$$

where $L_K = (\nu^3/\varepsilon)^{1/4}$ is the Kolmogorov scale. The dimensionless numbers in equations (3), (4) and (5) are related by

$$Fr_T = \frac{Fr_\gamma}{Re_T^{1/2}} \tag{6}$$

One final length scale used in discussing the laboratory and numerical results below is the Ellison scale L_E defined as

$$L_E = -\frac{\left(\overline{\rho'^2}\right)^{1/2}}{\frac{\partial \bar{\rho}}{\partial z}} \tag{7}$$

where ρ is the mean density and ρ' the fluctuating density. Itsweire et al. (1993) demonstrated that, with the exception of flows with very high mean Richardson numbers when the turbulence is not active, L_C and L_E can be taken as the same scale for practical purposes, as we do below.

As the turbulence associated with the initial pulse spectra used to initiate the DNS calculations becomes self-adjusted for dimensionless times St > 2 (Holt et al., 1992), all results quoted here were computed by ensemble-averaging the data from the 128^3 computational domain for St > 2. In general the sources of turbulence for driving the mixing will come from both turbulence associated with the initial conditions and that generated by the mean shear, but both these possible contributions are captured by computing R_f according to the definition in (2). Note that while the turbulence therefore evolved from the initial values as the calculations proceeded, by construction the mean flow Richardson number Ri remained constant for all times.

Mixing Efficiency

The buoyancy flux b is given by

$$b = \frac{g}{\rho_0}\overline{\rho' w'} = \frac{g}{\rho_0} R_{\rho w} \overline{\rho'} \overline{w'} \tag{8}$$

where $R_{\rho w}$ is the correlation coefficient and $\overline{\rho'}$ and $\overline{w'}$ are the rms values of the density and vertical velocity fluctuations, respectively. Now writing

$$\overline{\rho'} = f_1 \frac{\rho_0}{g} N^2 L_C \tag{9}$$

$$\overline{w'} = f_2 \varepsilon^{1/3} L_C^{1/3} \tag{10}$$

where f_1 and f_2 are unknown functions which could potentially be dependent on Ri and t as well as the method of computation of $\overline{\rho'}$ and $\overline{w'}$ (see below), then substituting (8), (9) and (10) into the definition of R_f in (2) yields

$$R_f = \frac{1}{1 + \dfrac{Fr_T^2}{R_{\rho w} f_1 f_2}} \tag{11}$$

As discussed above, rather than use L_C we use the length scale L_E in (9) and (10) and thus, by the definition in (7), the corresponding function $f_1 = 1$. In order to determine f_2, in Figure 1a we plot $\overline{w'}$ against $(\varepsilon L_E)^{1/3}$ for the current DNS results for all Pr, while in Figure 1b we show the corresponding results from the earlier laboratory studies discussed by Ivey and Imberger (1991). Data in both figures cover a wide range of Fr_T, from the energetic turbulence case with $Fr_T > 1$ to the buoyancy controlled regime with $Fr_T < 1$. For comparison, in Figure 1a we include the best fit line of $\overline{w'} = 0.82\,(\varepsilon L_E)^{1/3}$ and in Figure 1b the best fit line of $\overline{w'} = 0.87\,(\varepsilon L_E)^{1/3}$. Included in the laboratory data in Figure 1b are also data points where the buoyancy flux is zero (these data were not included in the best fit). It is interesting to note that these points always lie *above* the best fit straight line, implying that there is likely some contamination of the measured velocities by internal waves (cf. Itsweire and Helland, 1989). Briggs et al. (1998) have recently argued that the contributions of internal wave-induced velocities is likely only felt when Ri is large - and certainly larger than for the runs plotted in Figure 1a which includes only active mixing cases with Ri equal to either 0.075 or 0.21.

If the linear correlations in Figures 1a and 1b hold in general, then it is consistent with the observations reported by Yamazaki (1990) of good agreement between his observed velocity spectrum and the Nasmyth spectrum, and hence good estimates of the dissipation, even in the limiting cases where the buoyancy flux was zero. In summary, providing that the turbulence is active, which in the present context we take as the requirement that $Re_T = (L_C/L_K)^{4/3} > 1$ (i.e. there exists a range of overturning velocity scales from L_K out to L_C), the data in Figure 1 suggests that if we use the length scale L_E then we may take $f_2 \approx 1$. Note, however, that for field data obtained from vertical casts, for example, where only L_C is available the value of the parameters f_1 and f_2 must be determined in order to use (11).

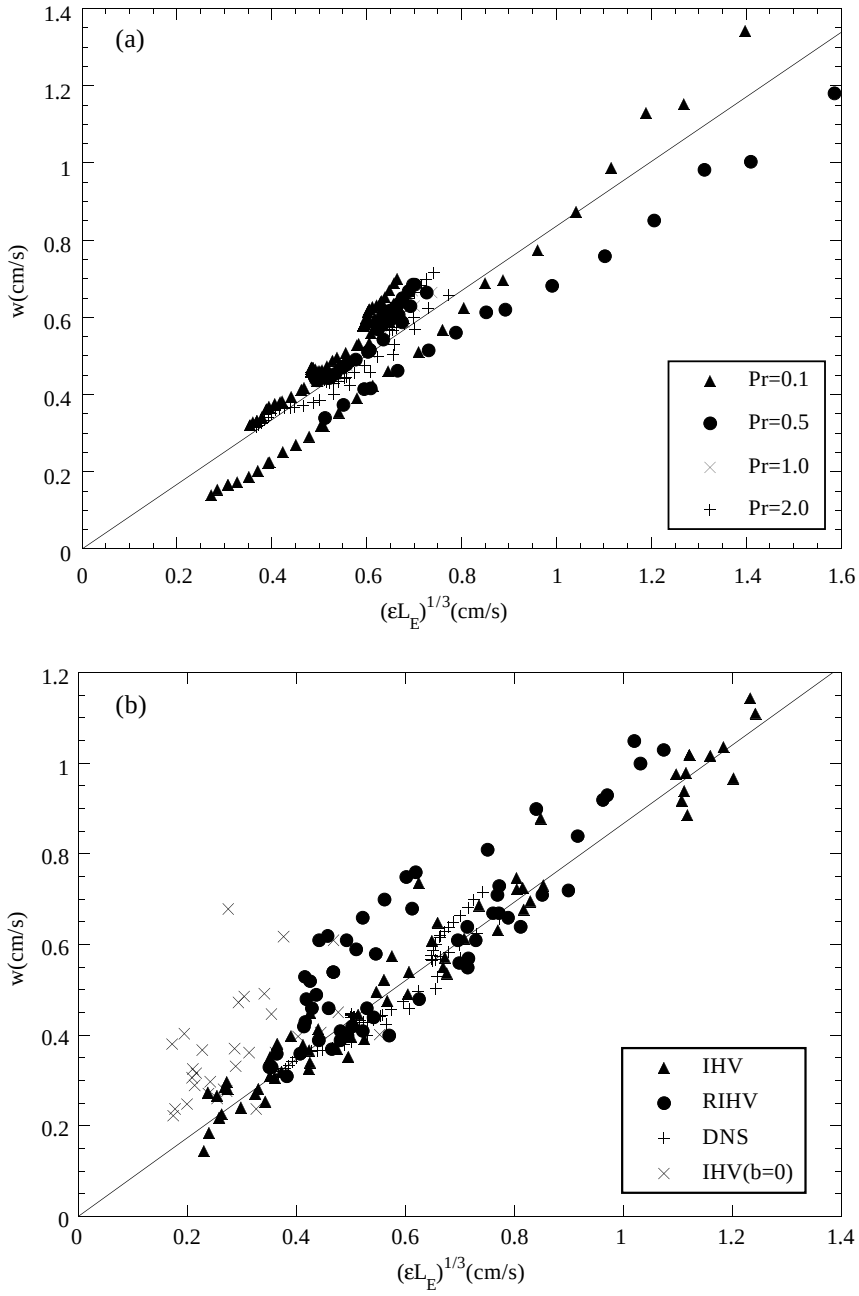

Figure 1. Vertical turbulent velocity as a function of overturning lengthscale and dissipation. Data sources are Itsweire et al. (1986) (IHV), Rohr et al. (1988) (RIHV), current numerical results (DNS). (a) DNS data (b) laboratory data

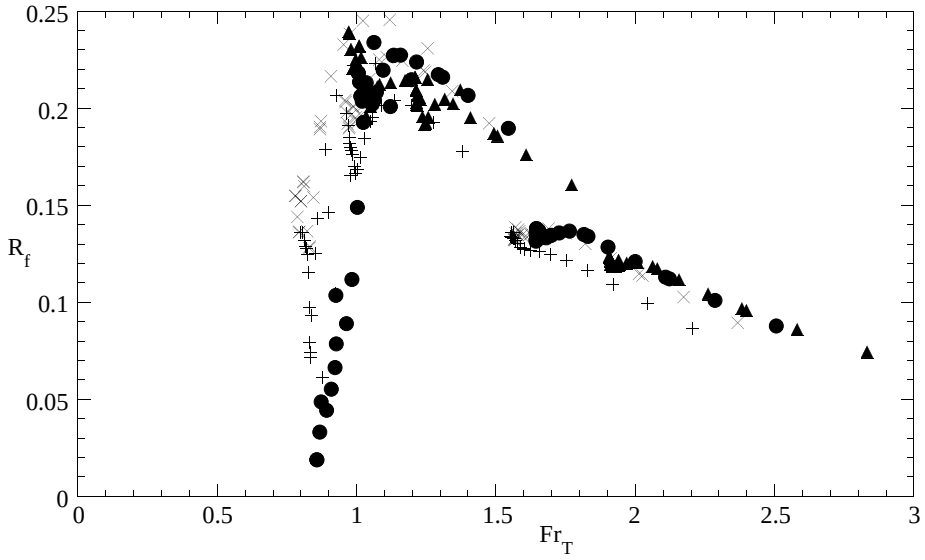

Figure 2. Mixing efficiency as a function of Froude number for the DNS results. Symbols are defined in Figure 1a.

The prediction in (11) can be tested against the numerical results and in Figure 2 we plot mixing efficiency R_f against Fr_T for the DNS runs with Pr = 0.1, 0.5, 1.0 and 2, all included. In the lower limit of $Fr_T \Rightarrow 0$, buoyancy completely suppresses all turbulence and $R_f = 0$. As Fr_T increases, R_f increases rapidly to reach a peak value near $Fr_T \approx 1$ and then decreases again with increasing Fr_T. Very large Fr_T is associated with vanishingly small N and this absence of a density gradient again causes R_f to become vanishingly small. Peak mixing efficiency of $R_f \approx 0.25$ for all runs, irrespective of Pr, is achieved between these two extremes at a value of Fr_T near 1. It is interesting to note from the form of equation (11) that, as the maximum allowable value of $R_{\rho w}$ is 1, the implied maximum achievable value of R_f is 0.5.

In their field observations of a stratified shearing flow, Seim and Gregg (1995) did not measure buoyancy flux directly but did estimate the mixing efficiency $R_f = 0.22$ when Fr_T lay in the range 0.85 to 1.3 (their Figure 3), clearly consistent with the numerical results in Figure 2 above. More recently, Lemckert and Imberger (1998) reported direct measurements of the buoyancy flux and R_f in the sloping benthic boundary layer of a lake and found good agreement with the form of the distribution shown in Figure 2. While the R_f distribution is also similar to the form found by Ivey and Imberger (1991) from laboratory data, the difference lies in the peak value of R_f reported in the earlier study, but clearly not evident in Figure 2. In particular, the peak value of $R_f = 0.15$ measured in the experiments with air at Pr = 0.7 is clearly smaller than observed in Figure 2 where the data span this value of Pr. Clearly the issue requires further investigation to resolve the causes of these apparent differences.

The use of (11) requires the specification of $R_{\rho w}$ and in Figure 3 we plot $R_{\rho w}$ as a function of Fr_T for all four Prandtl numbers from the DNS results. For $Fr_T > 1$, the density and vertical velocity fluctuations are strongly correlated with $R_{\rho w}$ in the range 0.2 - 0.6, independent of Fr_T. Ivey and Imberger (1991) suggested $R_{\rho w} = 0.3$ was a best estimate for

the laboratory data and Weinstock (1992) has argued on the basis of a theoretical model that $R_{\rho w} = 0.26$. Taking all these observations into account, we thus take $R_{\rho w} = 0.4$ as the asymptotic value and for the range $Fr_T > 1$ write (11) as

$$R_f = \frac{1}{1+2.5\ Fr_T^2} \tag{12}$$

which is in good agreement with the observations in Figure 2. Note that in the limit of $Fr_T = 1$ equation (12) predicts $R_f = 0.28$. This value is consistent with the results shown in Figure 2 and while apparently larger than some laboratory estimates, we adopt (12) here as it is conservative in predicting an upper bound for R_f and hence for buoyancy flux.

The expression in (12) cannot always hold since as the turbulence weakens viscosity must start to become important at some point. To investigate this, we show in Figure 4 the dependence of $R_{\rho w}$ on $\varepsilon/\nu N^2$. Ivey et al. (1993) discussed some earlier DNS results for $Pr < 1$ which indicated that both the value of $R_{\rho w}$ and the transition value of the parameter $\varepsilon/\nu N^2$ which sustained a positive buoyancy flux decreased with decreasing Pr. With the application to limnology and oceanography in mind, we discuss here only the case for $Pr > 1$. In Figure 4 we show the results for the DNS runs with $Pr = 2$ and, for comparison, also the laboratory data from Itsweire et al. (1986) and Rohr et al. (1988) in salt stratified fluids with $Pr = 700$. The data sets indicate that $\varepsilon/\nu N^2 = 15$ is a good estimate of the lower limit which sustains a positive buoyancy flux. Note also that $R_{\rho w}$ is constant only for $\varepsilon/\nu N^2 > 75$. Thus given the relation in (6), along the transition line where $Fr_T = 1$ the value of R_f is given by (12) for $Re_T \geq 75$, but in the range $15 < Re_T < 75$ must decrease with reducing values of Re_T to the limit of $R_f = 0$ when $Re_T \leq 15$.

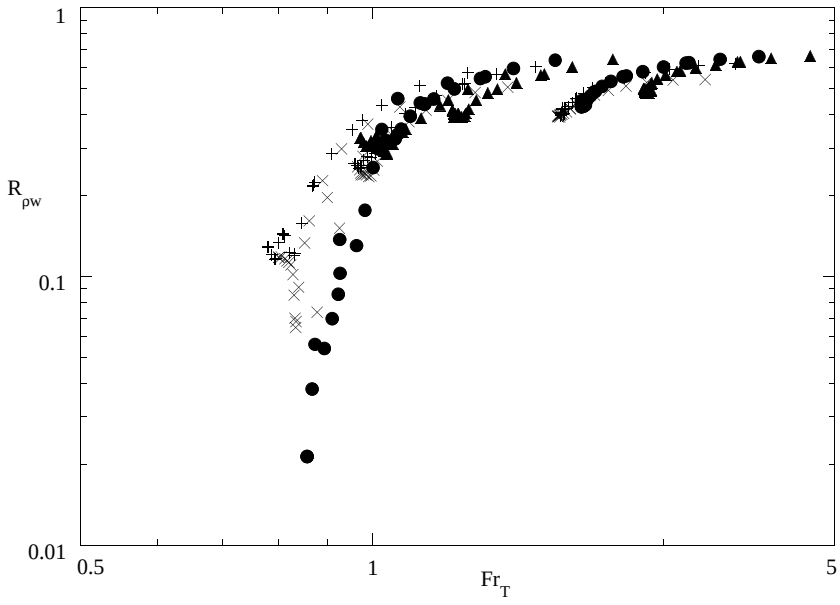

Figure 3. Correlation coefficient as a function of Froude number. Symbols are defined in Figure 1a.

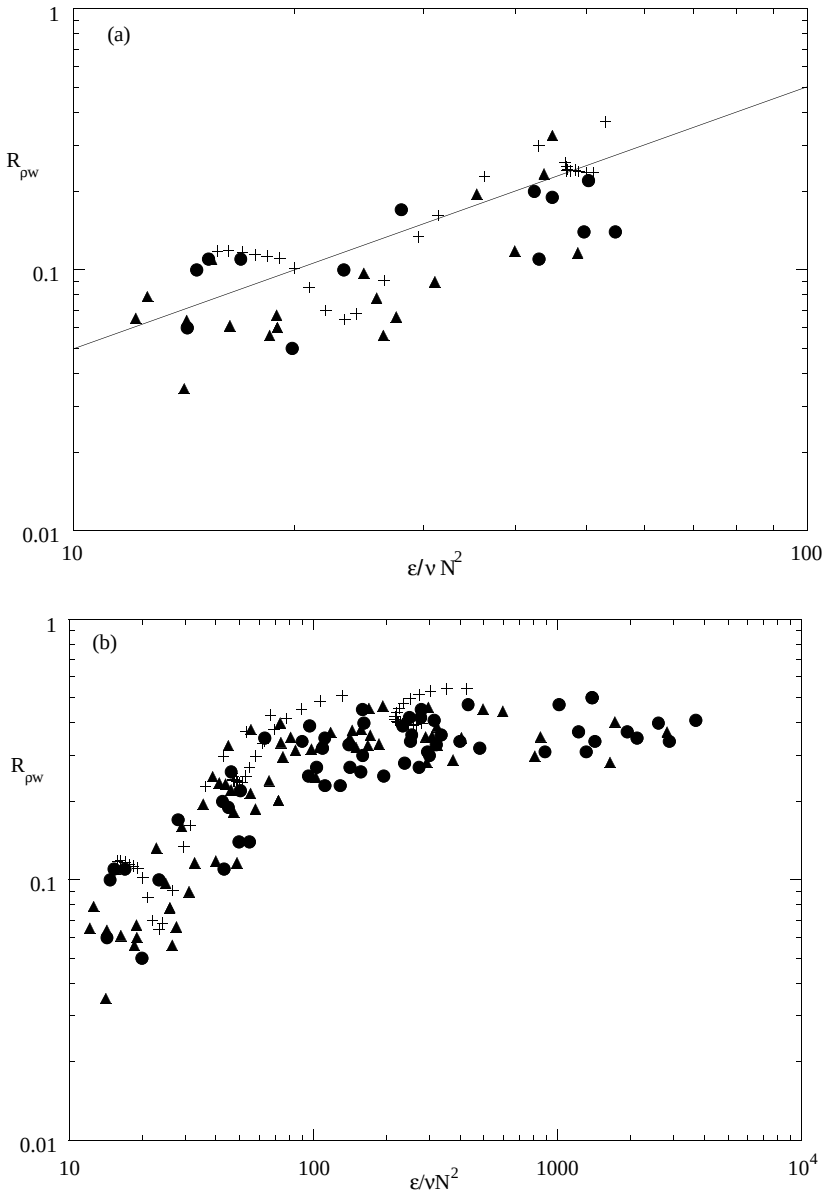

Figure 4. Correlation coefficient as a function of $\varepsilon/\nu N^2$. Symbols are defined in Figure 1a. (a) $Fr_T < 1$ (best fit shown: $R_{\rho w} = 0.0059\ (\varepsilon/\nu N^2)^{0.91}$ (b) All Fr_T.

As Figure 3 shows, for the regime where $Fr_T < 1$, the correlation coefficient $R_{\rho w}$ is not a constant and in fact rolls off very strongly with decreasing Fr_T. For these less active regimes, even combining the data from the numerical and laboratory results the data sets

are clearly limited and more data, most likely obtainable in the field, is needed. However, we do know the behaviour of the mixing efficiency R_f in the two limits. Firstly, we know that the buoyancy flux and hence $R_f = 0$ when $Fr_\gamma = (\varepsilon/\nu N^2)^{1/2} = 15^{1/2}$. Secondly, in the upper limit when $Re_T \geq 75$ and $Fr_T = 1$ we have from (12) that $R_f = 0.28$. These two limiting conditions are satisfied by the interpolation given by

$$R_f = 0.28\left(\frac{Fr_\gamma - \sqrt{15}}{\sqrt{Re_T} - \sqrt{15}}\right) \tag{13}$$

Discussion

The arguments above imply that a number of regimes in Fr_T - Re_T parameter space are possible. In Figure 5 and Table 1, we summarise the results for the various regimes described above for the case of $Pr > 1$. In regime 3 where $Fr_T > 1$ and $Re_T > 75$, R_f is given by (12). In regime 2, we modify this by taking a simple linear interpolation between the

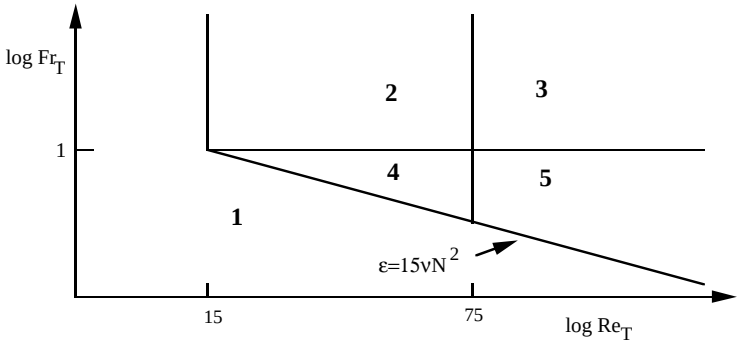

Figure 5. Froude number versus Reynolds number diagram with regimes marked.

TABLE 1. Regimes for Pr>1.

Regime	R_f
1	0
2	$R_f = \left(\frac{Re_T - 15}{60}\right)\frac{1}{1 + 2.5\ Fr_T^2}$
3	$R_f = \frac{1}{1 + 2.5\ Fr_T^2}$
4	$R_f = 0.0047\ (Re_T - 15)\left(\frac{Fr_\gamma - \sqrt{15}}{\sqrt{Re_T} - \sqrt{15}}\right)$
5	$R_f = 0.28\left(\frac{Fr_\gamma - \sqrt{15}}{\sqrt{Re_T} - \sqrt{15}}\right)$

upper limit given by (12) applied at $Re_T = 75$ and the lower limit of $R_f = 0$ when $Re_T = 15$. In regime 5 where $Fr_T < 1$ and $Re_T > 75$, R_f is given by (13). In regime 4, where $Fr_T < 1$ and $15 \le Re_T \le 75$, we again use a linear interpolation between (13) evaluated at the right hand boundary where $Re_T = 75$, and the requirement that $R_f = 0$ along the lower boundary where $\varepsilon/\nu N^2 = 15$ (the diagonal line in Figure 5). In regime 1 the value of $R_f = 0$ everywhere. For each regime, the expressions for R_f are summarized in Table 1, and the buoyancy flux can then be obtained directly from the definition in (2) which can be rearranged to yield $b = \varepsilon R_f/(1-R_f)$.

The model regimes depicted in Figure 5 and described in Table 1 are intended to provide simple yet complete formulae for the computation of R_f and buoyancy flux b which are as consistent as possible with available data and are conservative in the sense of predicting upper bounds on quantities. The underlying model extends or differs from previous work in several aspects. Unlike other studies (e.g., Schumann and Gerz, 1995), the model is applicable to both mechanically generated and shear generated turbulence. Unlike other studies (e.g., Weinstock, 1992) it makes no assumptions about the spectral forms or growth rates of the turbulence. Finally, the present model explicitly incorporates the effect of viscosity in defining a series of regimes which describe the mixing efficiency R_f, and hence buoyancy flux b, down to and including the limit where the combined action of buoyancy and viscosity suppress the vertical buoyancy fluxes. Such strongly buoyancy controlled situations occur both in the stratified ocean (e.g., Yamazaki, 1990) and in stratified lakes (e.g., Imberger and Ivey, 1991).

Acknowledgment. This work was supported by the Australian Research Council.

References

Briggs, D. A., J. H. Ferziger, J. R. Koseff, and S. G. Monismith, Turbulent mixing in a shear-free stably stratified two-layer fluid, *J. Fluid Mech., 354*, 175-208, 1998.

Gibson, C. H., Fossil temperature, salinity and vorticity in the ocean. *Marine turbulence*, edited by J. Nihoul, Elsevier, 221-258, 1980.

Gibson, C. H., Kolmogorov similarity hypotheses for scalar fields: sampling intermittent turbulent mixing in the ocean and galaxy, in *Turbulence and Stochastic Processes: Kolmogorov's ideas 50 years on,* edited by J. C. R. Hunt, O. M. Phillips and D. Williams, pp. 149-164. The Royal Society, London, 1991.

Gregg, M. C., Diapycnal mixing in the thermocline: A review. *J. Geophys. Res*., *92*, 5249-5286, 1987.

Holt, S. E., J. R. Koseff, and J. H. Ferziger, A numerical study of the evolution and structure of homogeneous stably stratified shear turbulence. *J. Fluid Mech., 237*, 499-540, 1992.

Imberger, J. and G. N. Ivey, On the nature of turbulence in a stratified fluid. Part II: Application to lakes. *J. Phys. Oceanogr., 21*, 659-680, 1991.

Itsweire, E. C., K. N. Helland and C. W. Van Atta, The evolution of grid-generated turbulence in a stratified fluid. *J. Fluid Mech., 126*, 299-338, 1986.

Itsweire, E. C. and K. N. Helland, Spectra and energy transfer in stably stratified turbulence. *J. Fluid Mech., 207*, 419-439, 1989.

Itsweire, E. C., J. R. Koseff, D. A. Briggs, and J. H. Ferziger, Turbulence in stratified shear flows: implications for interpreting shear-induced mixing in the ocean. *J. Phys Oceanogr., 23*, 1508-1522, 1993.

Ivey, G. N. and J. Imberger, On the nature of turbulence in a stratified fluid. Part I: The energetics of mixing, *J. Phys. Oceanogr., 21*, 650-658, 1991.

Ivey, G. N., J. Koseff, D. Briggs, and J. H. Ferziger, Mixing in a stratified shear flow: energetics and sampling. *Annual Research Briefs - 1992, Centre for Turbulence Research*, Stanford University, 335-344, 1993.

Lemckert, C. and J. Imberger, The benthic boundary layer, in *Physical Processes in Lakes and Oceans*, edited by J. Imberger, Coastal and Estuarine Studies, pp. 485-498, this volume, 1988.

Lienhard, J. H. and C. W. Van Atta, The decay of turbulence in thermally stratified flow. *J. Fluid Mech., 210*, 57-112, 1990.

Pacanowski, R. C. and S. G. H. Philander, Parameterization of vertical mixing in numerical models of the tropical ocean. *J. Phys. Oceanogr., 11*, 1443-1451, 1981.

Rohr, J. J., E. C. Itsweire and C. W. Van Atta, Mixing efficiency in stably-stratifed decaying turbulence, *Geophys. Astrophys. Fluid Dyn., 29*, 2211-236, 1984.

Rohr, J. J., E. C. Itsweire, K. N. Helland and C. W. Van Atta, An investigation of the growth of turbulence in a uniform-mean-shear flow. *J. Fluid Mech., 187*, 1-33, 1988.

Schumann, U. and T. Gerz, Turbulent mixing in stably stratified shear flows. *J. Appl. Meteorology, 34*, 33-48, 1995.

Seim, H. E. and M. C. Gregg, Energetics of a naturally occurring shear instability. *J. Geophys. Res., 100*, 4943-4958, 1995.

Stillinger, D. C., K. N. Helland and C. W. Van Atta, Experiments on the transition of homogeneous turbulence to internal waves in a stratified fluid. *J. Fluid Mech., 131*, 91-122, 1983.

Yamazaki, H. Stratified turbulence near a critical dissipation rate. *J. Phys Oceanogr., 20*, 1584-1598, 1990.

Weinstock, J. Vertical diffusivity and overturning length in stably stratified turbulence. *J. Geophys. Res. 8*, 12653-12658, 1992.